Chemical Engineering Journal 157 (2010) 401–407

Contents lists available at ScienceDirect

Chemical Engineering Journal

journal homepage: www.elsevier.com/locate/cej

Strontium and calcium ion adsorption by molecularly imprinted hybrid gel

Quan Li[a], Haining Liu[a,b], Tengyun Liu[a,b], Min Guo[a,b], Binju Qing[a,b], Xiushen Ye[a,b], Zhijian Wu[a,c,*]

[a] Key Laboratory of Salt Lake Resources and Chemistry, Qinghai Institute of Salt Lakes, Chinese Academy of Sciences, Xining 810008, China
[b] Graduate University of Chinese Academy of Sciences, Beijing 100049, China
[c] The Key Laboratory for Functional Materials of Fujian Higher Education, College of Materials Science and Engineering, Huaqiao University, Quanzhou 362021, China

ARTICLE INFO

Article history:
Received 20 December 2008
Received in revised form
10 November 2009
Accepted 23 November 2009

Keywords:
Strontium
Calcium
Adsorption
Hybrid gel
Molecular imprinting

ABSTRACT

The adsorption of strontium and calcium ions by strontium ion-imprinted hybrid gel derived from bis(trimethoxysilylpropyl)amine (TSPA) was comparatively studied. The effects of initial solution pH, ionic strength, initial metal ion concentration, and temperature on the equilibrium adsorption amount and the separation factor between strontium and calcium ions were comprehensively investigated. In description of the adsorption kinetics, the pseudo second-order model was found to be more suitable than the pseudo first-order model. In general, the equilibrium adsorption amount of both Sr^{2+} and Ca^{2+} ions was found to increase with the increase in both the initial metal ion concentration and pH, but not to be so sensitive to ionic strength and temperature. The separation of Sr^{2+} and Ca^{2+} ions could rely on the difference in adsorption kinetics, because Sr^{2+} ions were found to adsorb more rapidly than Ca^{2+} ions at the early adsorption stage.

© 2009 Elsevier B.V. All rights reserved.

1. Introduction

Strontium-90 is one of the most abundant radionuclides in nuclear fission products that are routinely or accidentally released. It has relatively long half-life of about 28.8 years and is a hazardous element for the environment [1]. Separation of strontium from alkaline and alkaline-earth elements is particularly important in the determination of the radioactive isotopes of strontium $^{89,90}Sr$ in natural samples. Isotopes $^{89,90}Sr$ are pure β-emitters and are difficult to be determined without separating strontium from natural and artificial radioactive isotopes [2].

Common strontium compounds in natural environments are important resources for the preparation of various kinds of strontium products. During the preparation process, the separation of strontium from co-existing elements, such as magnesium, calcium, sodium, and potassium is very important.

Several techniques have been developed for the separation of strontium to date. Originally, strontium was efficiently separated from large quantities of calcium and sodium as well as from a number of other elements by sedimentation with fuming nitric acid [2]. To avoid the use of fuming nitric acid due to its toxicity and aggressiveness, other techniques have been developed such as the isolation with ion exchangers and extraction agents [3–6]. However, in the development of these techniques a problem arises regarding the separation of strontium from calcium due to their similar chemical behavior. Furthermore, the simultaneous separation of a number of interfering elements such as sodium, iron, natural and artificial isotopes (^{137}Cs, ^{40}K) and many other elements is also a problem [2].

Adsorption has become one of the most commonly used separation methods due to its simplicity, selectivity, and efficiency [7]. Although there have been some reports on the adsorption of calcium [8–10] or strontium ions [2,11–29], a comprehensive study on the adsorptive separation of strontium from calcium ions is still required.

In adsorptive separation, good adsorbents are crucial for the separation. Efficient adsorbents should possess stable and insoluble porous matrices and suitable active groups (typically organic groups) that interact with the adsorbates, such as metal ions. Silica-based hybrid gels or modified silica gels are promising adsorbent candidates because of their good chemical, mechanical, and thermal stability [30]. Immobilization and cross-linking of organic compounds onto the surfaces of silica gels have gained important applications in different research and industrial fields [31–35]. The effectiveness of such materials in binding metal ions has been attributed to the complexation between the ligands and the metal ions. Although such materials have been used as metal ion adsorbents, their selectivity is not so good [36].

Molecular imprinting, a technique of tailor-making network materials for the recognition of specific analyte molecules, has attracted increasing interest in recent years [37,38]. For metal ions, molecular imprinting can be described more precisely as ionic

---

[*] Corresponding author at: Key Laboratory of Salt Lake Resources and Chemistry, Qinghai Institute of Salt Lakes, Chinese Academy of Sciences, 18 Xinning Rd., Xining, Qinghai 810008, China. Tel.: +86 971 6307871; fax: +86 971 6307871.
E-mail address: zjw6512@hotmail.com (Z. Wu).

1385-8947/$ – see front matter © 2009 Elsevier B.V. All rights reserved.
doi:10.1016/j.cej.2009.11.029

imprinting. This technique may improve the adsorbent selectivity significantly. Some metal ion-imprinted polymers have been used for metal ion adsorption, such as Cr(III) [39], Ni(II) [40–42], Cu(II) [43], Cd(II) [44,45], Zn(II) [46], Pd (II) [47], Dy(III) [48], UO_2(II) [49], Mg(II) [50], Ca(II) [51], and Fe(III) [52] imprinted polymers. However, no imprinted adsorbents were reported for the adsorption of strontium ions. In this study, strontium ion-imprinted hybrid gel was prepared by the sol–gel technique. The obtained gel was used to adsorb strontium and calcium ions from aqueous solutions. The effects of initial solution pH, ionic strength, metal ion concentration, and temperature on the adsorption were comprehensively investigated.

2. Materials and methods

2.1. Gel preparation

The strontium ion-imprinted hybrid gel was prepared through a one-step sol–gel process. Bis(trimethoxysilylpropyl)amine (TSPA, Gelest) was used as the gel precursor. 600 mL of 1.2 mol L^{-1} $SrCl_2$ aqueous solution was mixed with 120 mL TSPA under stirring. After gelation, the gel was aged for one day. The aged gel was dried at 30 °C for two days, and the dried gel was ground and sieved. The gel with a particle size between 830 and 350 μm was selected for the removal of the imprinting strontium ions and then used for the adsorption. The imprinting strontium ions in the gel were removed by treating the gel with 0.1 mol L^{-1} EDTA solution for three times. Then the gel was treated with 2 mol L^{-1} ammonia for three times, followed by washing several times with pure water until the pH of the water became ~7. The wet gel particles were stored and used for the adsorption experiments.

2.2. Adsorption experiments

In the adsorption kinetic experiments, 4 g of the wet gel particles were dispersed in 200 mL solution at the desired initial $SrCl_2$ or $CaCl_2$ concentration (4, 8, and 12 mmol L^{-1}). No HCl, NaOH, or NaCl was added to adjust the solution pH or ionic strength.

In the adsorption thermodynamic experiments, 0.2 g of the wet gel particles were dispersed in 10 mL solution at the desired initial $SrCl_2$ or $CaCl_2$ concentration, pH, and ionic strength. Solution pH was adjusted with dilute HCl or NaOH solutions and ionic strength was controlled with NaCl solution. The adsorption time was fixed at two days. Except for the experiments on adsorption isotherms, the adsorption temperature was 20 °C. In the experiments about the effect of initial solution pH on the adsorption, no NaCl solution was added to adjust the solution ionic strength. In the experiments about the effect of ionic strength on the adsorption, no HCl or NaOH solution was added to adjust the solution pH.

All the adsorption experiments were carried out using a SHA-C shaking water bath (Changzhou Guohua Co., Ltd., P.R. China) with a shaking speed of 80 rpm at the desired temperature. After adsorption, the supernatant was used to determine the concentration of Sr^{2+} or Ca^{2+} ions with the complex titration method using eriochrome black T or calcium indicator as an indicator. The solution pH was adjusted with $NH_4Cl–NH_3·H_2O$ buffer solution or NaOH solution. The amount of Sr^{2+} or Ca^{2+} adsorbed onto the particles (q, in millimoles per gram of the dried particles) was calculated by a mass balance relationship:

$$q = \frac{V(C_0 - C)}{W} \tag{1}$$

where C_0 and C are Sr^{2+} or Ca^{2+} concentration in solution before and after adsorption (mmol L^{-1}). V is the volume of the solutions (L). W is the dry weight of the gel particles used (g). When C_e is used instead of C in Eq. (1), q_e can be obtained.

The adsorption amount was calculated based on the dry weight of the gel particles. The dry weight of the gel particles was calculated by considering the water content of the wet gel particles. The water content of the wet gel particles was determined by the weight change before and after drying of the gel particles at 30 °C, which was found to be 54.5%.

The distribution coefficient (D) and the separation factor ($\beta^{Sr}{}_{Ca}$) between Sr^{2+} and Ca^{2+} ions were calculated according to the following two equations:

$$D = \frac{q_e}{C_e} \tag{2}$$

$$\beta^{Sr}_{Ca} = \frac{D_{Sr}}{D_{Ca}} \tag{3}$$

where D_{Sr} and D_{Ca} are the distribution coefficients of Sr^{2+} and Ca^{2+} ions, respectively.

3. Results and discussion

3.1. Time for the adsorption equilibrium

Figs. 1 and 2 show the amount of adsorbed Sr^{2+} and Ca^{2+} ions as a function of time, respectively. As shown in Figs. 1 and 2, adsorption occurs rapidly in the first 2 h, after which the adsorbed amount changes slowly. According to these results, the time for the adsorption experiments was fixed at two days to make sure that equilibrium was reached. For the adsorption of Sr^{2+} ions by zeolite A, previous studies indicated that 80–90% of the equilibrium amount was adsorbed within 30 min. The initial rapid adsorption was followed by the slow approach to equilibrium, and equilibrium was reached in 90–120 min [16].

The high adsorption rate in the beginning may be due to the fact that initially all sites on the surfaces of the gel particles are vacant and the metal ion concentration gradient is high. As the adsorption continues, the number of vacant sites and the concentration gradient decrease, resulting in the decrease in the adsorption rate [16].

Figs. 1 and 2 also show that the adsorption reaches equilibrium more rapidly at a higher temperature. The initial metal ion concentration does not have a significant effect on the adsorption equilibrium time.

To show the differences in the adsorption kinetics between Sr^{2+} and Ca^{2+} more clearly, the relationship between the separation factor $\beta^{Sr}{}_{Ca}$ and the adsorption time was shown in Fig. 3. In general, the separation factor is based on the adsorption equilibrium data, here it is calculated based on the data before adsorption equilibrium only to show the adsorption differences between Sr^{2+} and Ca^{2+} ions more clearly. Fig. 3 shows that Sr^{2+} ions are adsorbed more rapidly than Ca^{2+} ions at the initial adsorption stage. Such a difference in adsorption kinetics may be used for practical separation.

3.2. Pseudo first- and second-order kinetic analyses

Both the pseudo first- and second-order adsorption models were tested against the adsorption kinetic data [53–55]. In both models, all the steps of adsorption including external diffusion, internal diffusion, and adsorption were lumped together. It was also assumed that the driving force for the adsorption was the difference between the average solid phase concentration and the equilibrium concentration, and that the overall adsorption rate was proportional to either the driving force (as in the pseudo first-order equation) or the square of the driving force (as in the pseudo second-order equation).

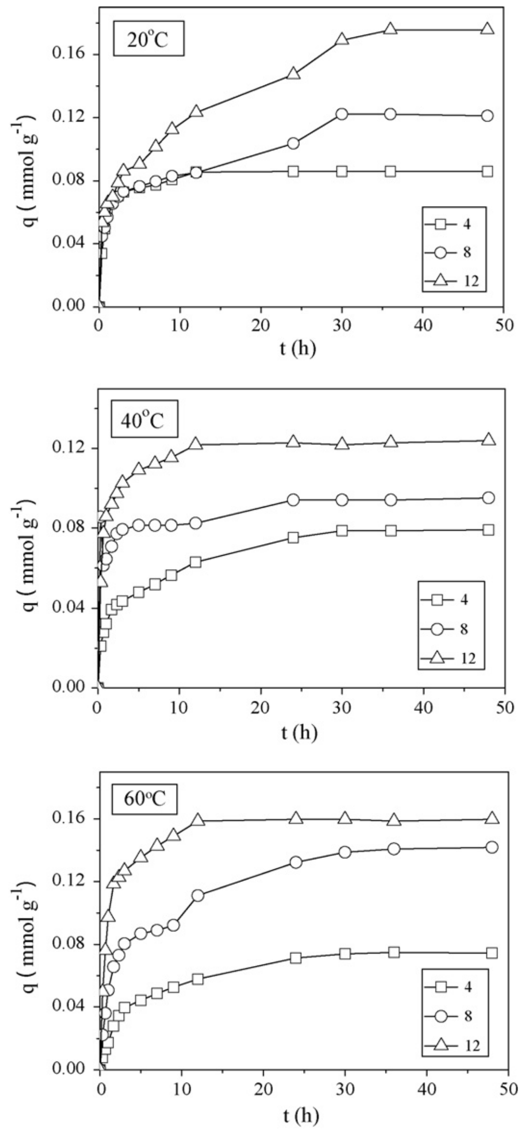

Fig. 1. Adsorption kinetic curves for Sr^{2+} ions under different initial Sr^{2+} concentrations ($mmol\,L^{-1}$).

Linear form equations:

$$\text{First-order model}: \ln(q_e - q_t) = \ln q_e - k_1 t \quad (4)$$

$$\text{Second-order model}: \frac{t}{q_t} = \frac{1}{k_2 q_e^2} + \frac{t}{q_e} \quad (5)$$

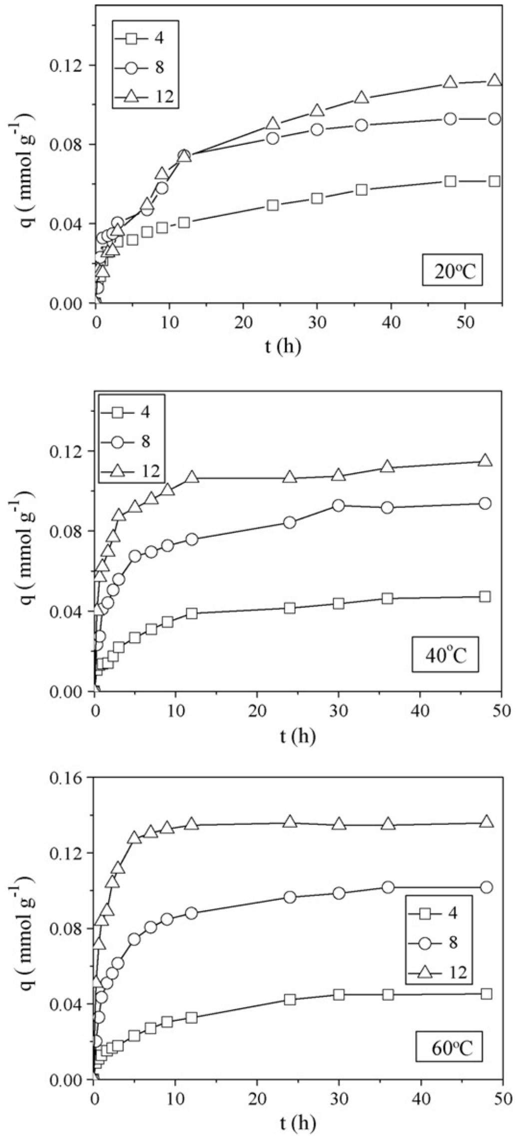

Fig. 2. Adsorption kinetic curves for Ca^{2+} ions under different initial Ca^{2+} concentrations ($mmol\,L^{-1}$).

Non-linear form equations:

$$\text{First-order model}: q_t = q_e - \frac{q_e}{e^{k_1 t}} \quad (6)$$

$$\text{Second-order model}: q_t = \frac{k_2 q_e^2 t}{1 + k_2 q_e t} \quad (7)$$

Table 1
Adsorption kinetic parameters for Sr^{2+} ions.

C_0 (mmol L^{-1})	T (°C)	$q_{e,exp}$ (mmol g^{-1})	First-order			Second-order		
			$q_{e,cal}$ (mmol g^{-1})	k (h^{-1})	r^2	$q_{e,cal}$ (mmol g^{-1})	k (g $mmol^{-1}$ h^{-1})	r^2
4.0	20	0.086	0.081 ± 0.002	1.28 ± 0.13	0.963	0.086 ± 0.001	24.0 ± 1.17	0.995
	40	0.079	0.070 ± 0.040	0.39 ± 0.08	0.843	0.077 ± 0.003	6.85 ± 1.30	0.933
	60	0.074	0.071 ± 0.003	0.22 ± 0.03	0.960	0.080 ± 0.002	3.46 ± 0.29	0.989
8.0	20	0.122	0.099 ± 0.006	0.72 ± 0.20	0.745	0.109 ± 0.006	8.24 ± 2.25	0.860
	40	0.095	0.087 ± 0.002	1.37 ± 0.21	0.923	0.092 ± 0.002	25.6 ± 3.64	0.972
	60	0.141	0.127 ± 0.007	0.31 ± 0.06	0.890	0.141 ± 0.006	2.89 ± 0.46	0.957
12.0	20	0.173	0.154 ± 0.011	0.25 ± 0.06	0.780	0.169 ± 0.011	2.24 ± 0.58	0.875
	40	0.123	0.115 ± 0.003	1.40 ± 0.18	0.942	0.122 ± 0.001	17.8 ± 1.22	0.991
	60	0.159	0.151 ± 0.003	0.93 ± 0.09	0.964	0.162 ± 0.001	8.48 ± 0.44	0.995

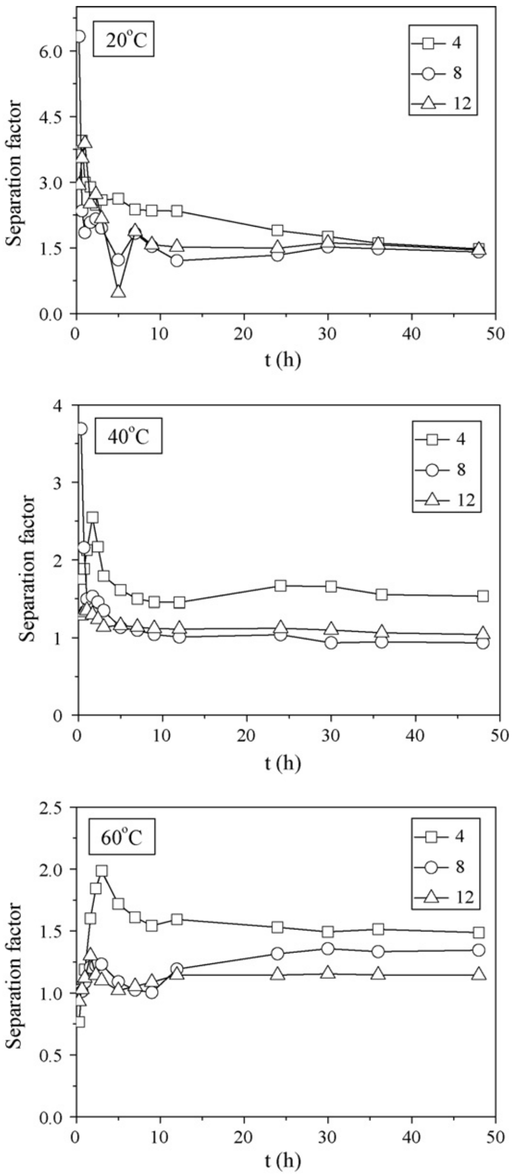

Fig. 3. The relationship between separation factor β_{Ca}^{Sr} and adsorption time under different initial metal ion concentrations (mmol L^{-1}).

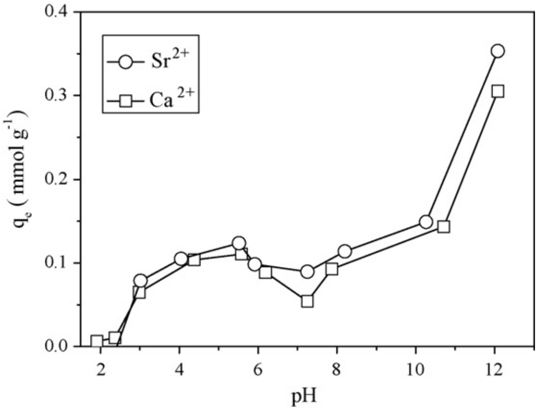

Fig. 4. Effect of initial solution pH on the equilibrium adsorption amount.

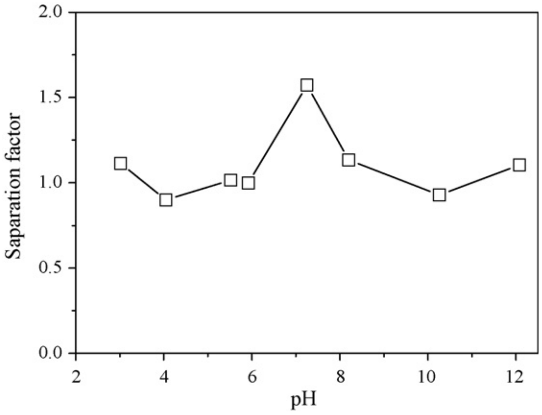

Fig. 5. Effect of initial solution pH on the separation factor.

In the above equations, q_t and q_e are the adsorption amount at time t and at equilibrium, and k_1 and k_2 are the adsorption rate constant for pseudo first- and second-order models, respectively. For the linear form of the first-order model, an experimentally determined equilibrium adsorption amount ($q_{e,exp}$) is required for the fitting, but $q_{e,exp}$ is often difficult to determine due to the slow adsorption processes. In this work, the non-linear equations of both first- and second-order were applied to test the experimental data.

The fitting results are given in Tables 1 and 2. According to the correlation coefficients, the second-order model is more suitable to describe the adsorption kinetic data than the first-order model. This is consistent with the previous works on the adsorption of Ca^{2+} ions onto kraft pulps [8] and Sr^{2+} onto zeolite A [16], where the adsorption was also found to follow a second-order kinetics.

3.3. *Effect of initial solution pH on the equilibrium adsorption amount*

The effects of initial solution pH on the equilibrium adsorption amount and the separation factor are shown in Figs. 4 and 5,

Table 2
Adsorption kinetic parameters for Ca^{2+} ions.

C_0 (mmol L^{-1})	T (°C)	$q_{e,exp}$ (mmol g^{-1})	First-order			Second-order		
			$q_{e,cal}$ (mmol g^{-1})	k (h^{-1})	r^2	$q_{e,cal}$ (mmol g^{-1})	k (g mmol^{-1} h^{-1})	r^2
4.0	20	0.061	0.052 ± 0.003	0.26 ± 0.05	0.857	0.058 ± 0.003	6.08 ± 1.16	0.934
	40	0.046	0.044 ± 0.002	0.22 ± 0.03	0.942	0.049 ± 0.002	5.67 ± 0.77	0.969
	60	0.045	0.043 ± 0.002	0.17 ± 0.02	0.935	0.049 ± 0.002	4.29 ± 0.64	0.965
8.0	20	0.092	0.087 ± 0.004	0.18 ± 0.03	0.918	0.097 ± 0.004	2.52 ± 0.45	0.956
	40	0.093	0.084 ± 0.003	0.43 ± 0.07	0.920	0.092 ± 0.002	6.32 ± 0.73	0.975
	60	0.102	0.094 ± 0.003	0.43 ± 0.05	0.950	0.103 ± 0.002	5.67 ± 0.39	0.991
12.0	20	0.108	0.106 ± 0.004	0.11 ± 0.01	0.973	0.127 ± 0.004	0.91 ± 0.11	0.986
	40	0.110	0.103 ± 0.003	0.85 ± 0.12	0.925	0.110 ± 0.002	11.7 ± 1.10	0.983
	60	0.135	0.131 ± 0.003	0.91 ± 0.10	0.957	0.139 ± 0.002	10.5 ± 0.75	0.990

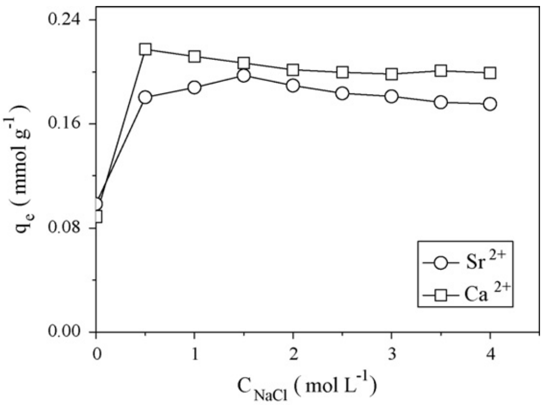

Fig. 6. Effect of ionic strength on the equilibrium adsorption amount.

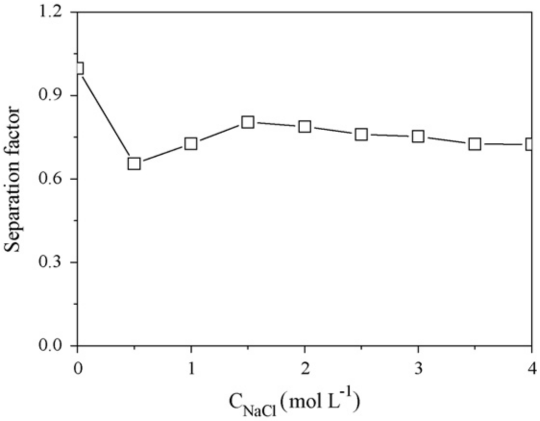

Fig. 7. Effect of ionic strength on the separation factor.

respectively. In general, the equilibrium adsorption amount of both Sr^{2+} and Ca^{2+} increases with pH in the pH range from 2 to 12. The separation factor shows a peak at pH about 7.0. The prepared gel adsorbents are hybrid gels with silica as the matrix and –NH– groups as the functional groups. According to the chemical composition of the gels, the gels are sensitive to solution pH. At low pH values, the metal ion uptake is inhibited in the acidic solutions and this can be attributed to the presence of H^+ ions competing with the metal ions for the adsorption sites. Another possibility is that at low pH the –NH– groups on the surface of the gels are fully protonated to form $-NH_2Cl-$ groups, unable to complex with Sr^{2+} or Ca^{2+} ions. At low pH values, the adsorption of both Sr^{2+} and Ca^{2+} ions are suppressed, and their adsorption behavior difference is weakened.

In this study, the uptake generally increases continuously with the increase in pH. Strontium and calcium could form mono-valent ionic pairs such as $SrCl^+$, $SrOH^+$ $CaCl^+$, $CaOH^+$ before being adsorbed [8]. At pH above ∼11.0, the obvious increase in adsorption was caused by the precipitation of $Sr(OH)_2$ and $Ca(OH)_2$, not by the real adsorption. At high pH, the adsorption behavior difference is also weakened due to hydroxide precipitate formation. Therefore, the adsorption behavior difference is more likely to appear at pH about 7.0.

The adsorption amount was also found to increase with pH values in the previous works: the adsorption of strontium ions by hydrous metal oxides [1], carbon materials [13], and zeolite A [16], and the adsorption of calcium ions by oxidized carboxymethyl starch and cross-linked carboxymethyl starch [10].

3.4. Effect of ionic strength on the equilibrium adsorption amount

The effect of ionic strength on the equilibrium adsorption amount is shown in Fig. 6. The adsorption of both Sr^{2+} and Ca^{2+} is not sensitive to ionic strength as NaCl concentration changes from 0.5 to 4 mol L^{-1}, suggesting that inner-sphere complexation reactions account for the adsorption and that there is a covalent bonding between the metal ions and the gel particles. For the adsorption of Sr^{2+} to hydrous ferric oxide (HFO), adsorption was also found to be insensitive to ionic strength [17]. In contrast, for strontium adsorption to hydrous aluminum and manganese oxides [1], cellulose/alginic acid ion-exchange membrane [11], and bacteria *Shewanella alga* [17], adsorption was found to decrease with increasing ionic strength, suggesting physical adsorption where hydrating waters were not lost upon adsorption and the outer-sphere complexation reactions accounted for the adsorption [17].

The effect of ionic strength on the separation factor is shown in Fig. 7. It is found that the separation factor is not sensitive to ionic strength.

3.5. Effect of initial metal ion concentration and temperature on the equilibrium adsorption amount—adsorption isotherms

The adsorption isotherms for the adsorption of Sr^{2+} and Ca^{2+} ions from aqueous solutions onto the gel particles were determined. The adsorption isotherms are shown in Fig. 8. It is clear that the adsorption amount of both ions generally increases with the increase in initial metal ion concentration. The increase in the uptake capacity of the gel particles with increasing initial ion concentration may be due to higher probability of collision between ions and the gel particles [16] and higher concentration gradient which increases mass transfer rate.

In this study, the adsorption amount of both Sr^{2+} and Ca^{2+} ions at equilibrium is not sensitive to temperature. However, for the adsorption of strontium by hydrous aluminum, iron, and man-

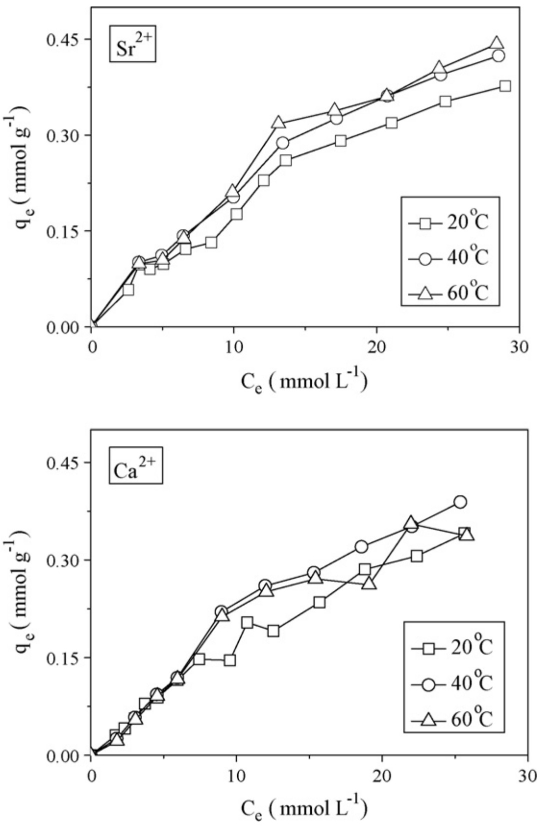

Fig. 8. Adsorption isotherms.

Table 3
Langmuir and Freundlich isotherm constants at different temperatures.

	T (°C)	Langmuir			Freundlich		
		q_m (mmol g^{-1})	K_L (L mmol^{-1})	r^2	K_F	$1/n$	r^2
Sr^{2+}	20	0.88 ± 0.12	0.027 ± 0.005	0.984	0.034 ± 0.004	0.73 ± 0.04	0.974
	40	0.91 ± 0.08	0.031 ± 0.004	0.995	0.042 ± 0.005	0.69 ± 0.04	0.985
	60	0.96 ± 0.13	0.031 ± 0.007	0.986	0.043 ± 0.008	0.70 ± 0.06	0.970
Ca^{2+}	20	0.88 ± 0.11	0.024 ± 0.004	0.990	0.028 ± 0.003	0.78 ± 0.03	0.986
	40	0.92 ± 0.16	0.029 ± 0.007	0.986	0.034 ± 0.006	0.76 ± 0.07	0.970
	60	0.71 ± 0.16	0.038 ± 0.013	0.964	0.036 ± 0.009	0.72 ± 0.09	0.934

ganese oxides, strontium adsorption was found to increase with increasing adsorption temperature [1]. For the adsorption of Ca^{2+} ions by unbleached kraft fibres [8], oxidized carboxymethyl starch and cross-linked carboxymethyl starch [10], the adsorption was found to decrease with the increase in temperature.

There are several isotherm models, which can be used to describe the equilibrium nature of adsorption [56]. However, adsorption mechanisms in solution are so complicated that no simple theory can adequately represent all experimental data. Most of the isotherm models used to describe adsorption in solution are based on semiempirical equations. In this study, the most widely used Langmuir and Freundlich equations in the following were tested against the experimental data:

$$\text{Langmuir model}: q_e = \frac{K_L q_m C_e}{1 + K_L C_e} \qquad (8)$$

$$\text{Freundlich model}: q_e = K_F C_e^{1/n} \qquad (9)$$

In the above equations, q_m is the adsorption capacity and K_L is the adsorption intensity or Langmuir coefficient. $1/n$ is the heterogeneity factor of the adsorbent and K_F is the Freundlich equation constant. The above non-linear Langmuir and Freundlich equations are used to fit the experimental data. The corresponding isotherm constants are listed in Table 3. The Langmuir isotherm was found to be more suitable to describe the adsorption isotherms. For the adsorption of Ca^{2+} ions onto kraft pulps [8], and the adsorption of Sr^{2+} onto zeolite A [16], the adsorption isotherms were also found to follow the Langmuir equation.

The effect of initial metal ion concentration and temperature on the separation factor is shown in Fig. 9. The separation factor is not sensitive to adsorption temperature. The initial metal ion concentration does not have any significant effect on the separation factor at initial metal ion concentration between 6 and 30 mmol L^{-1}, even though it is higher at low initial metal ion concentration (4 mmol L^{-1}).

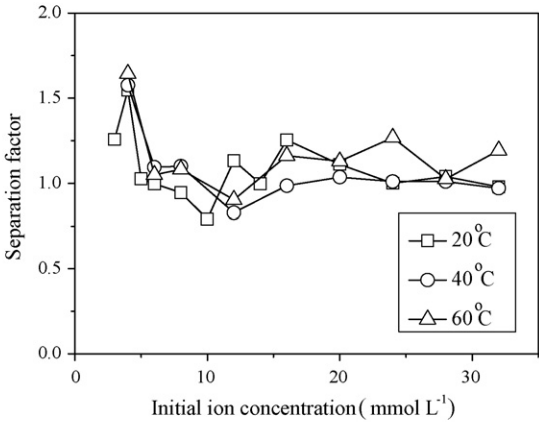

Fig. 9. Effect of initial metal ion concentration and temperature on the separation factor.

According to the experimental data, the adsorption of Sr^{2+} and Ca^{2+} ions onto the strontium ion-imprinted hybrid gel shows a similar behavior, meaning that the separation between Sr^{2+} and Ca^{2+} ions is not so satisfactory. Thus, the simple ion-imprinting technique is not so effective to achieve the selective adsorption of Sr^{2+} ions. However, the separation may be achieved or improved through (1) utilizing the difference in initial adsorption rate; (2) preparing better adsorbents using a composite imprinting technique; (3) designing the preferential desorption process.

4. Conclusions

The use of strontium ion-imprinted hybrid gel for the adsorption of both Sr^{2+} and Ca^{2+} ions from aqueous solutions has been investigated. The results are summarized as follows:

(1) The adsorption of both Sr^{2+} and Ca^{2+} ions occurs rapidly in the first 2 h, after which the adsorption amount changes slowly. The adsorption reaches equilibrium more rapidly at a higher temperature. The initial metal ion concentration does not have any significant effect on the adsorption equilibrium time. The pseudo second-order model is more suitable to describe the adsorption kinetic data than the pseudo first-order model. Sr^{2+} ions are adsorbed more rapidly than Ca^{2+} ions at the initial adsorption stage, which may be used for the separation of Sr^{2+} and Ca^{2+} ions.
(2) The equilibrium adsorption amount of both Sr^{2+} and Ca^{2+} ions increases with the increase in both the initial metal ion concentration and pH, but is not so sensitive to ionic strength and temperature. The Langmuir equation is more suitable to describe the adsorption isotherms than the Freundlich equation.
(3) In general, the separation factor between Sr^{2+} and Ca^{2+} ions is not so sensitive to initial solution pH, ionic strength, and adsorption temperature. Thus, the separation of Sr^{2+} and Ca^{2+} ions cannot easily be enhanced using the equilibrium process. A composite imprinting technique should be employed to improve the preparation of the adsorbent.

Acknowledgments

This work was financially supported by the foundation of National Natural Science Foundation of China (50972151), Knowledge Innovation Program of Chinese Academy of Sciences (kzcx2-yw-115), Natural Science Foundation of Fujian Province, China (No. E0710016), and Hundred Talent Program of Chinese Academy of Sciences (0660011106).

References

[1] P. Trivedi, A. Lisa, A comparison of strontium sorption to hydrous aluminum, iron, and manganese oxides, J. Colloid Interf. Sci. 218 (1999) 554–563.
[2] Ž. Grahek, I. Eškinja, K. Košutic, S. Lulic, K. Kvastek, Isolation of radioactive strontium from natural samples: separation of strontium from alkaline and

alkaline earth elements by means of mixed solvent anion exchange, Anal. Chim. Acta 379 (1999) 107–119.

[3] T. Kimura, K. Iwashima, T. Ishimori, T. Hamada, Separation of strontium-89 and -90 from calcium in milk with a macrocyclic ether, Anal. Chem. 51 (1979) 1113–1116.

[4] E.P. Horwitz, M.L. Dietz, D.E. Fisher, Separation and preconcentration of strontium from biological, environmental, and nuclear waste samples by extraction chromatography using a crown ether, Anal. Chem. 63 (1991) 522–525.

[5] S.B. Clark, Separation and determination of radiostrontium in calcium carbonate materials of biological origin, J. Radioanal. Nucl. Chem. (Articles) 194 (1995) 297–302.

[6] M. Pimpl, 89Sr/90Sr-determination in soils and sediments using crown ethers for Ca/Sr-separation, J. Radioanal. Nucl. Chem. (Articles) 194 (1995) 311–318.

[7] E.-D. Hwang, K.-W. Lee, K.-H. Choo, S.-J. Choi, S.-H. Kim, C.-H. Yoon, C.-H. Lee, Effect of precipitation and complexation on nanofiltration of strontium-containing nuclear wastewater, Desalination 147 (2002) 289–294.

[8] T.D. Duong, K.L. Nguyen, M. Hoang, Competitive sorption of Na$^+$ and Ca^{2+} ions on unbleached kraft fibres-A kinetics and equilibrium study, J. Colloid Interf. Sci. 301 (2006) 446–451.

[9] V.E. Badillo-Almaraz, J. Ly, Calcium sorption on hydroxyapatite in aqueous solutions: reversible and nonreversible components, J. Colloid Interf. Sci. 258 (2003) 27–32.

[10] Y.-X. Chen, G.-Y. Wang, Adsorption properties of oxidized carboxymethyl starch and cross-linked carboxymethyl starch for calcium ion, Colloid Surf. A 289 (2006) 75–83.

[11] L. Zhang, J. Zhou, D. Zhou, Y. Tang, Adsorption of cadmium and strontium on cellulose/alginic acid ion-exchange membrane, J. Membrane Sci. 162 (1999) 103–109.

[12] O. Chiyoda, M.E. Davis, Adsorption studies with gmelinite zeolites containing mono-, di- and tri-valent cations, Micropor. Mesopor. Mater. 38 (2000) 143–149.

[13] R.A. Shawabkeh, D.A. Rockstraw, R.K. Bhada, Copper and strontium adsorption by a novel carbon material manufactured from pecan shells, Carbon 40 (2002) 781–786.

[14] M.V. Sivaiah, K.A. Venkatesan, R.M. Krishna, P. Sasidhar, G.S. Murthy, Ion exchange properties of strontium on in situ precipitated polyantimonic acid in amberlite XAD-7, Sep. Purif. Technol. 44 (2005) 1–9.

[15] A. Zhang, E. Kuraoka, M. Kumagai, Development of the chromatographic partitioning of cesium and strontium utilizing two macroporous silica-based calix[4]arene-crown and amide impregnated polymeric composites: PREC partitioning process, J. Chromatogr. A 1157 (2007) 85–95.

[16] A.M. El-Kamash, Evaluation of zeolite A for the sorptive removal of Cs$^+$ and Sr^{2+} ions from aqueous solutions using batch and fixed bed column operations, J. Hazard. Mater. 151 (2008) 432–445.

[17] T.D. Small, L.A. Warren, F.G. Ferris, Influence of ionic strength on strontium sorption to bacteria, Fe(III) oxide, and composite bacteria-Fe(III) oxide surfaces, Appl. Geochem. 16 (7–8) (2001) 939–946.

[18] L. Axe, T. Tyson, P. Trivedi, T. Morrison, Local structure analysis of strontium sorption to hydrous manganese oxide, J. Colloid Interf. Sci. 224 (2000) 408–416.

[19] G. Gürboğa, H. Tel, Preparation of TiO_2–SiO_2 mixed gel spheres for strontium adsorption, J. Hazard. Mater. B 120 (2005) 135–142.

[20] W. van Beinum, A. Hofmann, J.C.L. Meeussen, R. Kretzschmar, Sorption kinetics of strontium in porous hydrous ferric oxide aggregates. I. The Donnan diffusion model, J. Colloid Interf. Sci. 283 (2005) 18–28.

[21] A. Hofmann, W. van Beinum, J.C.L. Meeussen, R. Kretzschmar, Sorption kinetics of strontium in porous hydrous ferric oxide aggregates. II. Comparison of experimental results and model predictions, J. Colloid Interf. Sci. 283 (2005) 29–40.

[22] N. Lua, C.F.V. Mason, Sorption––desorption behavior of strontium-85 onto montmorillonite and silica colloids, Appl. Geochem. 16 (2001) 1653–1662.

[23] C.A. Papachristodoulou, P.A. Assimakopoulos, N.-H.J. Gangas, Strontium adsorption properties of an aluminum-pillared montmorillonite carrying carboxylate functional groups, J. Colloid Interf. Sci. 245 (2002) 32–39.

[24] J. Tits, E. Wieland, C.J. Müller, C. Landesman, M.H. Bradburya, Strontium binding by calcium silicate hydrates, J. Colloid Interf. Sci. 300 (2006) 78–87.

[25] O.N. Karasyova, L.I. Ivanova, L.Z. Lakshtanov, L. Lövgren, Strontium sorption on hematite at elevated temperatures, J. Colloid Interf. Sci. 220 (1999) 419–428.

[26] I.D. Smičiklas, S.K. Milonjić, P. Pfendt, S. Raičević, The point of zero charge and sorption of cadmium (II) and strontium (II) ions on synthetic hydroxyapatite, Sep. Purif. Technol. 18 (2000) 185–194.

[27] M.N. Pace, M.A. Mayes, P.M. Jardine, L.D. McKay, X.L. Yin, T.L. Mehlhorn, Q. Liu, H. Gürleyük, Transport of Sr^{2+} and SrEDTA^{2-} in partially-saturated and heterogeneous sediments, J. Contam. Hydrol. 91 (2007) 267–287.

[28] N. Sahai, S.A. Carroll, S. Roberts, P.A. O'Day, X-ray absorption spectroscopy of strontium (II) coordination. II. Sorption and precipitation at kaolinite, amorphous silica, and goethite surfaces, J. Colloid Interf. Sci. 222 (2000) 198–212.

[29] T. Möller, R. Harjula, J. Lehto, Ion exchange of ^{85}Sr, ^{134}Cs and ^{57}Co in sodium titanosilicate and the effect of crystallinity on selectivity, Sep. Purif. Technol. 28 (2002) 13–23.

[30] P.K. Jal, S. Patel, B.K. Mishra, Chemical modification of silica surface by immobilization of functional groups for extractive concentration of metal ions, Talanta 62 (2004) 1005–1028.

[31] S.M. Seo, E.J. Cho, S.J. Lee, K.C. Nam, S.-H. Park, J.H. Jung, A mesoporous silica functionalized by a covalently bound naphthalene-based receptor for selective optical detection of fluoride ion in water, Micropor. Mesopor. Mater. 114 (2008) 448–454.

[32] J. Fan, C. Wu, Y. Wei, C. Peng, P. Peng, Preparation of xylenol orange functionalized silica gel as a selective solid phase extractor and its application for preconcentration—separation of mercury from waters, J. Hazard. Mater. 145 (2007) 323–330.

[33] R. Brambilla, G.P. Pires, J.H.Z.d. Santos, M.S.L. Miranda, B. Chornik, Octadecylsilane-modified silicas prepared by grafting and sol–gel methods, J. Electron. Spectrosc. Relat. Phenom. 156–158 (2007) 413–420.

[34] D.E. Leyden, G.H. Luttrell, Preconcentration of trace metals using chelating groups immobilized via silylation, Anal. Chem. 47 (1975) 1612–1617.

[35] R. Kocjan, M. Garbacka, Additional purification of alkaline earth salts by using silica gel modified with pyrocatechol violet as a sorbent, Talanta 41 (1994) 131–133.

[36] M.E. Mahmoud, A.A. Soayed, O.F. Hafez, Selective solid phase extraction and pre-concentration of heavy metals from seawater by physically and chemically immobilized 4-amino-3-hydroxy-2-(2-chlorobenzene)-azo-1-naphthalene sulfonic acid silica gel, Microchim. Acta 143 (2003) 65–70.

[37] V. Pichon, F. Chapuis-Hugon, Role of molecularly imprinted polymers for selective determination of environmental pollutants—a review, Anal. Chim. Acta 622 (2008) 48–61.

[38] P.A.G. Cormack, K. Mosbach, Molecular imprinting: recent developments and the road ahead, React. Funct. Polym. 41 (1999) 115–124.

[39] E. Birlik, A. Ersoz, E. Acikkalp, A. Denizli, R. Say, Cr(III)-imprinted polymeric beads: sorption and preconcentration studies, J. Hazard. Mater. 140 (2007) 110–116.

[40] S. Haijia, Z. Ying, L. Jia, T. Tianwei, Biosorption of Ni^{2+} by the surface molecular imprinting adsorbent, Process Biochem. 41 (2006) 1422–1426.

[41] A. Ersoz, R. Say, A. Denizli, Ni(II) ion-imprinted solid-phase extraction and preconcentration in aqueous solutions by packed-bed columns, Anal. Chim. Acta 502 (2004) 91–97.

[42] Q. Li, H. Su, J. Li, T. Tan, Application of surface molecular imprinting adsorbent in expanded bed for the adsorption of Ni^{2+} and adsorption model, J. Environ. Manage. 85 (2007) 900–907.

[43] R. Say, E. Birlik, A. Ersoz, F. Yilmaz, T. Gedikbey, A. Denizli, Preconcentration of copper on ion-selective imprinted polymer microbeads, Anal. Chim. Acta 480 (2003) 251–258.

[44] B. Gao, F. An, Y. Zhu, Novel surface ionic imprinting materials prepared via couple grafting of polymer and ionic imprinting on surfaces of silica gel particles, Polymer 48 (2007) 2288–2297.

[45] F. Li, H. Jiang, S. Zhang, An ion-imprinted silica-supported organic–inorganic hybrid sorbent prepared by a surface imprinting technique combined with a polysaccharide incorporated sol-gel process for selective separation of cadmium(II) from aqueous solution, Talanta 71 (2007) 1487–1493.

[46] K. Araki, T. Maruyama, N. Kamiya, M. Goto, Metal ion-selective membrane prepared by surface molecular imprinting, J. Chromatogr. B 818 (2005) 141–145.

[47] S. Daniel, J.M. Gladis, T.P. Rao, Synthesis of imprinted polymer material with palladium ion nanopores and its analytical application, Anal. Chim. Acta 488 (2003) 173–182.

[48] V.M. Biju, J.M. Gladis, T.P. Rao, Ion imprinted polymer particles: synthesis, characterization and dysprosium ion uptake properties suitable for analytical applications, Anal. Chim. Acta 478 (2003) 43–51.

[49] P. Metilda, J.M. Gladis, T.P. Rao, Influence of binary/ternary complex of imprint ion on the preconcentration of uranium(VI) using ion imprinted polymer materials, Anal. Chim. Acta 512 (2004) 63–73.

[50] P.K. Dhal, F.H. Arnold, Template-mediated synthesis of metal-complexing polymers for molecular recognition, J. Am. Chem. Soc. 113 (1991) 7417–7448.

[51] T. Rosatzin, L.I. Andersson, W. Simon, K. Mosbach, Preparation of Ca^{2+} selective sorbents by molecular imprinting using polymerisable ionophores, J. Chem. Soc., Perkin Trans. 2 (1991) 1261–1265.

[52] X. Chang, N. Jiang, H. Zheng, Q. He, Z. Hu, Y. Zhai, Y. Cui, Solid-phase extraction of iron(III) with an ion-imprinted functionalized silica gel sorbent prepared by a surface imprinting technique, Talanta 71 (2007) 38–43.

[53] L. You, Z. Wu, T. Kim, K. Lee, Kinetics and thermodynamics of bromophenol blue adsorption by a mesoporous hybrid gel derived from tetraethoxysilane and bis(trimethoxysilyl)hexane, J. Colloid Interf. Sci. 300 (2006) 526–535.

[54] Y.S. Ho, G. McKay, Pseudo-second order model for sorption processes, Process Biochem. 34 (1999) 451–465.

[55] Z. Wu, H. Joo, K. Lee, Kinetics and thermodynamics of the organic dye adsorption on the mesoporous hybrid xerogel, Chem. Eng. J. 112 (2005) 227–236.

[56] I.D. Mall, V.C. Srivastava, N.K. Agarwal, Removal of orange-G and methyl violet dyes by adsorption onto bagasse fly ash-kinetic study and equilibrium isotherm analyses, Dyes Pigment 69 (2006) 210–223.